Volumetric and transport properties in microemulsions and the point of view of percolation theory

S. K. Mehta* and Kiran Bala
Department of Chemistry, Panjab University, Chandigarh - 160014, India
(Received 23 September 1994)

Microemulsions have been prepared from either benzene, toluene, ethylbenzene, or *o*-xylene and water using a mixture of surfactants of Span 80 and Tween 20 in the volume ratio of 1:4. These formulated microemulsions having propanol as the cosurfactant have been characterized by measuring their dynamic properties, i.e., conductance σ, density ρ, viscosity η, and ultrasonic velocity u, as a function of the volume fraction of water ϕ at 30 °C. The conductance values change exponentially as the volume fraction of water is increased. The use of a percolation model gives reasonable agreement between the experimental and calculated values. The viscosities vary in a nonmonotonic way, giving two peaked plots when the water content increases, indicating a lack of correlation with conductivity. The ultrasonic velocity and isentropic compressibility K_S data throw some light on structural changes that occur in the microemulsion. An attempt has also been made to calculate the density ρ_m and isentropic compressibility $K_{S,m}$ of the micellar phase from the experimental data. The results indicate a trend toward an enhanced waterlike character of the dispersed phase at a high volume fraction of water ϕ.

PACS number(s): 82.70.Kj

I. INTRODUCTION

In the presence of a suitable combination of surfactant and a cosurfactant viz. an alkaline-earth-metal soap and a medium-chain-length alkanol, two immiscible liquids, e.g., water-and-oil-type organic liquids can form transparent and thermodynamically stable systems that have been labeled as microemulsions [1–4]. The process of emulsification is spontaneous and requires little or no mechanical agitation. Two types of microemulsions, water-in-oil (w-o) or Oil-in-water (o-w) can be obtained, the type being dependent on the chemical nature of the surface active agents and relative constituent properties.

During the last few years, different methods have been used to investigate these microemulsions with the help of many advanced techniques, e.g., low angle x-ray diffraction [5], light scattering [6], ultracentrifugation [7], electron microscopy [8], viscosity [9,10], conductance [11–14], and ultrasonic velocity [15]. Microemulsions are extraordinary solutions in some respects and, therefore, are considered promising in a number of important industrial applications [3,4].

With the progress of the studies on microemulsion, the knowledge of their structure has become inevitably important. Recently, we have reported [16] microemulsion systems containing Tween 20 as a surfactant component. The effect of salinity on the physical properties was investigated. Starting from the oil corner of the Gibb's triangle and proceeding towards the water rich side, the conductivity rises sharply by three to four orders of magnitude with increasing water content due to the percolation of water droplets [17].

The concept of percolation transition is often used in interpreting the conductivity of disordered systems. At fixed temperature T and ratio n_a/n_s, and for small droplet concentration (low ϕ), the interactions are so weak that the droplets may be regarded as an assembly of dynamical noninteracting isolated spheres dispersed in the continuum oil phase. However as ϕ increases the droplets may form dynamical random clusters that at sufficiently high ϕ, called the critical value of the volume fraction ϕ_c, may percolate into an infinite dynamic or static interconnected network.

The analyses of volumetric properties such as density and isentropic compressibility provide useful information on the structural conditions of the micellar phase at different ϕ. Similarly, the transport properties, such as static shear viscosity and electrical conductivity, enable one to characterize the role of the interdroplet connectivity due to attractive interactions.

In this paper, detailed measurement of volumetric (ρ, K_S) and transport (η, σ) properties of samples formulated by Span 80+Tween 20+propanol+oil (benzene-toluene-ethylbenzene-*o*-xylene) as a function of the volume fraction of water throughout the single phase region are presented. It has been observed that the conductivity values vary exponentionally as the water content is increased in the system displaying the percolation phenomenon. The viscosity in each system goes through two maxima and these do not consistently correlate with features of conductivity curves for the present set of microemulsions. Read and Healy [18] and Bennette *et al.* [19] have also noted this lack of correlation. Ultrasonic velocity values increase up to a point, move through a flattened maximum, and then start to decrease. The influence of the change of oil on the conductance, viscosity, and ultrasonic velocity have also been investigated.

II. EXPERIMENT

High grade benzene (Sisco Chem), toluene (Fluka Buchs), ethylbenzene (Fluka Buchs), *o*-xylene (Fluka

*Author to whom correspondence should be addressed.

Buchs), propanol (Merck), Span 80 (Kochlight Lab), and Tween 20 (Hi media Lab) and triply distilled water have been used to prepare the microemulsion samples. Microemulsion formulation with Span 80 is not possible as it does not dissolve in water but it is readily soluble in the aqueous solution of Tween 20. The microemulsions were prepared by mixing appropriate fractions of water, surfactant, cosurfactant, and hydrocarbon. A dilution series was obtained by fixing the ratio of the number of moles of alcohol to the number of moles of surfactant (n_a/n_s) as two and varying the volume fraction ϕ of water.

The conductivity σ was measured with a Digital conductivity meter (model NDC 732) of Naina Electronics (Cell constant = 11.7 m^{-1}). Measurements of viscosity were carried out using a suspended level dilution Ubbelohde capillary viscometer. During measurements, the viscometer was placed in a water bath thermostatted at 30.00±0.01 °C. The dynamic viscosity η was obtained from the kinematic viscosity data by multiplying by the density of the studied sample. The density ρ was measured with the help of a high precision Anton Paar automatic densimeter.

For the accurate ultrasonic velocity measurements, the ultrasonic time intervalometer (UTI-101) from Innovative instruments based on pulse-echo-overlap technique (PET) was used. A transducer of frequency 2 MHz was used for the measurement. All samples were characterized by the volume fraction of water ϕ and the experiments were performed at 30.0±0.01 °C. The experimental conductivity σ and viscosity η values are reported in Table I whereas Table II lists the data of density ρ and ultrasonic velocity u at 30 °C.

TABLE I. Conductivity (σ) and viscosity (η) of Span 80 + Tween 20 + benzene + propanol + water microemulsion as a function of the volume fraction of water (ϕ) at $T = 30$ °C.

ϕ	$\sigma 10^3$ ($S\,m^{-1}$)	η (cP)
0	0.168	19.468
0.0126	0.253	21.062
0.0248	0.343	
0.0368	0.419	23.145
0.0485	0.494	
0.0599	0.552	25.210
0.0710	0.604	
0.0819	0.622	28.369
0.0925	0.653	
0.1029	0.709	31.298
0.1129	0.783	
0.1278	0.944	33.043
0.1421	1.159	
0.1559	1.391	34.666
0.1693	1.631	
0.1823	1.885	35.299
0.1949	2.191	
0.2071	2.480	35.095
0.2189	2.855	
0.2342	3.346	34.249
0.2488	3.861	
0.2629	4.434	35.125
0.2765	4.984	
0.2896	5.522	35.802
0.3022	6.119	
0.3144	6.669	36.529
0.3262	7.289	
0.3376	7.851	37.676
0.3486	8.436	
0.3592	8.962	39.197
0.3695	9.524	
0.3795	10.039	44.811
0.3891	10.553	
0.3985	11.092	49.638
0.4119	11.735	
0.4249	12.390	53.691
0.4373	13.069	
0.4511	13.736	52.256
0.4659	14.461	
0.4801	15.093	43.764
0.4952	15.631	
0.5109	16.286	31.284
0.5257	16.965	26.336
0.5527		19.015
0.5985		11.60

III. RESULTS AND DISCUSSION

A. Conductivity studies

Figure 1 shows the plot of σ versus ϕ at constant temperature and molar ratio of alcohol to surfactant. Con-

TABLE II. Ultrasonic velocity (u) at 2 MHz, density (ρ), and compressibility values (K_S) calculated by the Laplace relation of Span 80 + Tween 20 + benzene + propanol + water microemulsion as a function of the volume fraction of water (ϕ) at $T = 30$ °C.

ϕ	u (ms^{-1})	ρ ($kg\,m^{-3}$)	K_S (TPa^{-1})
0	1414.9	989.6	504.7
0.0248	1431.6	994.3	490.9
0.0485	1448.7	998.5	477.5
0.0819	1466.4	1003.4	463.6
0.1129	1485.9	1007.5	449.5
0.1514	1507.1	1011.1	435.5
0.1949	1526.6	1014.4	423.2
0.2488	1546.9	1016.3	411.3
0.3022	1560.2	1017.4	403.9
0.3539	1573.2	1019.2	396.5
0.4030	1580.3	1019.3	392.9
0.4642	1586.9	1019.3	389.7
0.5139	1578.1	1019.3	394.1
0.5675	1569.9	1019.2	398.2
0.6199	1561.6	1019.2	402.4
0.6681	1553.7	1019.3	406.5
0.7054	1547.5	1019.3	409.8
0.7439	1541.7	1019.2	412.9
0.7735	1536.6	1019.2	415.7
0.8020	1532.6	1019.2	417.8
0.8242	1528.8	1019.1	419.9
0.8419	1526.5	1019.1	421.1

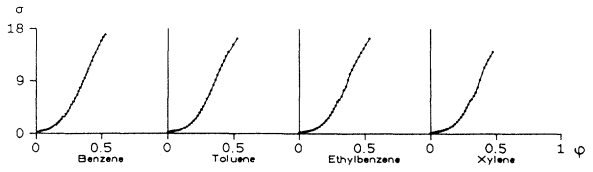

FIG. 1. Variations of the conductivity $10^3\sigma$ ($S\,m^{-1}$) vs volume fraction of water ϕ for the system water+(Span 80+Tween 20)+propanol+oil.

ductivity values vary exponentially with respect to volume fraction ϕ showing a transition from a low conductive region to a highly conductive region. This can be best discussed with the help of a percolation concept. The percolation transition signifies the first emergence of an infinite cluster of some critical value of volume fraction ϕ_c. There is a continuous transition at ϕ_c to a conducting state. Some other authors [11–14,20–23] have also observed similar results.

The influence of the change of the oil on the conductivity has also been investigated. As the oils are nonconducting in nature, the conductance values are not significantly affected by the change of the oil as shown in Fig. 1. The calculated value of the percolation threshold $\phi_c=0.14$ is the same for systems containing different oil, which confirms the above observation.

We have utilized a theoretical model of Grest *et al.* [12], which is based on the dynamic picture of percolation, to analyze the conductivity results of the present studies. A percolation picture for the transition involves the formation of clusters of water globules that are significantly close to each other. This results in an efficient transfer of charge carrier between the water globules [24,25]. An alternative view is that the formation of a continuous connected water phase is responsible for the conductivity transition [26]. The experimental results [27,28], together with theoretical arguments [12], provide additional support in favor of the former view. According to the theory

$$\sigma=\begin{cases}A(\phi_c-\phi)^{-s} & \text{if } \phi<\phi_c\ , \quad (1)\\ B(\phi-\phi_c)^{t} & \text{if } \phi>\phi_c\ . \quad (2)\end{cases}$$

Above the percolation transition ϕ_c, σ varies as Eq. (2). Experimental studies on dynamic microemulsion systems [20,24,27,29,30] and static systems [31,32] and theoretical studies [33,34] have shown that $t=1.2-2.1$. Equation (1), which is applicable below the percolation transition, i.e., $\phi<\phi_c$, is expected to diverge [34,35]. Grannan, Gailand, and Tanner [36] and Song *et al.* [31] have suggested $s=0.7$ for static systems. Peyrelasse and co-workers [9–11] have utilized $t=1.94$ and $s=1.2$ for the analysis of the conductivity of water-AOT-oil systems. We have obtained for the present set of systems the value of s as 2.5 and that of t as 1.36.

The above equations are valid only near ϕ_c and cannot be extrapolated to infinite dilution and unit concentration. Also, these are not applicable at the immediate vicinity of ϕ_c, where there is a continuous variation within a narrow interval around the percolation threshold.

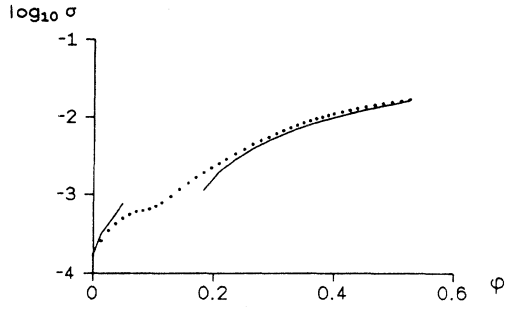

FIG. 2. Variations of $\log_{10}\sigma$ vs volume fraction of water ϕ. The line is the theoretical curve [Eqs. (1) and (2)]; the dots are the experimental data for water + (Span 80 +Tween 20)+propanol+benzene.

The analysis of our conductance results are shown in Fig. 2. There is a good agreement between calculated and experimental values over the whole range of composition with a mean deviation of 8.85%. The plot of $(1/\sigma)(d\sigma/d\phi)$ versus ϕ (Fig. 3) passes through a maximum giving the exact estimate of the magnitude of ϕ_c.

The present set of microemulsions are believed to be w-o type at low water concentrations. Below the percolation threshold ϕ_c, the water droplets are isolated from each other and contribute little to conductance. However, for the volume fraction of water above the percolation threshold ϕ_c, some of these conducting droplets begin to contact each other and form clusters, i.e., there exists a continuous path of water reaching from one side of the sample to the other. Hence the conductivity will start to increase rapidly from an almost zero value to a much higher value.

B. Density studies

Figure 4 displays the dependence of density ρ vs ϕ at constant temperature for the microemulsion system containing benzene as oil. It shows an increase continuously up to $\phi=0.35$ and then becomes almost constant. To ac-

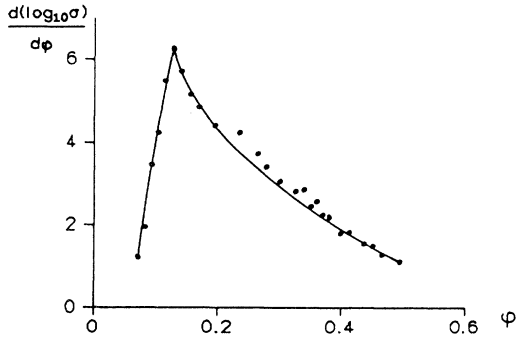

FIG. 3. Variations of $(d\log_{10}\sigma)/(d\phi)$ vs volume fraction of water ϕ for the system water+(Span 80+Tween 20)+propanol+benzene.

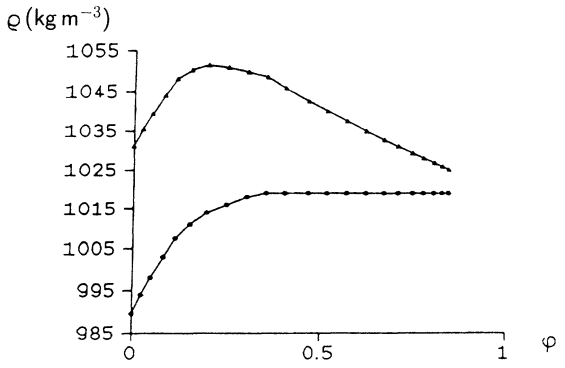

FIG. 4. Variations of density ρ (kg m^{-1}) vs volume fraction of water ϕ, micellar density ρ_m (▲) and experimental density (dotted line) for water+(Span 80+Tween 20)+propanol +benzene.

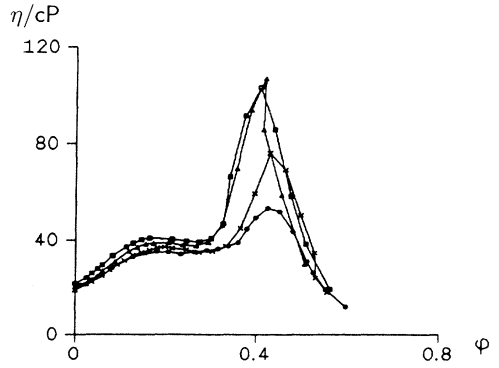

FIG. 5. Variations of η (cP) vs volume fraction of water ϕ for the system water+(Span 80+Tween 20)+propanol+oil, benzene (dotted line); toluene (x-x); ethylbenzene (▲); o-xylene (■).

count for the ϕ dependence of ρ, let us consider the role of the micellar phase. Assuming [37] the additivity of the volumes of the micellar and oil phase, one can attempt to evaluate the micellar density by the relation

$$\rho=\phi_m\rho_m+\phi_o\rho_o\ , \tag{3}$$

where ρ_o and ρ_m are the density of the oil and of the micellar phases, respectively. ϕ_o is the volume fraction of oil phase whereas $\phi_m=(1-\phi_o)$ represents the volume fraction of micellar phase.

Equation (3) considers the microemulsions as made by two separated nonintracting regions, one containing droplets and/or connected droplets and the other containing the oil phase. Plots of $(\rho-\phi_o\rho_o)$ vs ϕ show a linear trend, thereby indicating the validity of relation (3).

The calculated micellar densities from Eq. (3) at different ϕ are also shown in Fig. 4. It indicates that as ϕ increases, p_m decreases from about the surfactant density ($\rho_{\text{Span+Tween[1:4]}}=1070.0$ kgm^{-3}) towards the water value ($\rho_w=997.0$ kgm^{-3}), indicating an increased waterlike character of the reversed micelles. Similar observation has also been reported [38–40] by different groups.

C. Viscosity studies

The variation of the dynamic viscosity η as a function of the volume fraction of water is shown in Fig. 5. It is observed that it varies in a nonomontonic [18,41,42] way as the water content increases. Unlike the conductance results, the viscosity behavior produces a local maximum at two composition points. The change of oil in the present system does not affect the first peak in the viscosity curve but the second peak grows in the order benzene < toluene < o-xylene < ethylbenzene as shown in Fig. 5.

The viscosity results of microemulsions in the present study are quite different from those of conductivity. Some other groups have also reported similar results [18,19]. The first peak in the viscosity curve coincides with the water percolation threshold as determined by electrical conductivity. A slight minimum observed may be the result of possibly the rearrangement of rapidly growing droplets forming clusters. The second maxima occurs at a high volume fraction of water and on further increases in ϕ, reaches the bicontinuous stage, thus showing a sharp decrease after this maxima.

D. Ultrasonic velocity

The behavior of ultrasonic velocity is quite interesting. Figure 6 shows the variation of ultrasonic velocity u vs ϕ. The u increases sharply with the addition of water but this increase in u becomes less and less, corresponding to the first peak in the viscosity curve. The value of u starts decreasing at a point roughly correspondingly to the second viscosity peak. These results appear to indicate that the addition of water affects the aggregates of oil-surfactant-alcohol by transforming them into loosely packed aggregates. The ultrasonic velocity decreases with the addition of oil in the order benzene > toluene > ethyl benzene > xylene. This might be because of loose packing with the large size of hydrocarbon molecules.

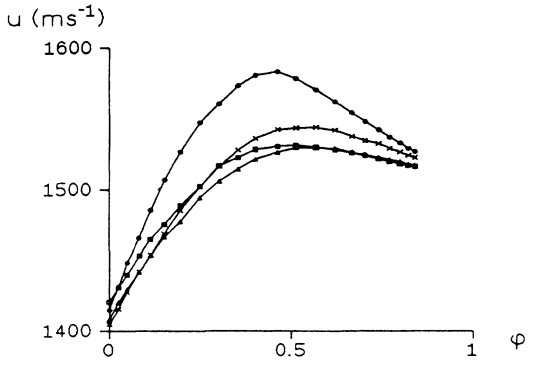

FIG. 6. Variations of the ultrasonic velocity u (ms^{-1}) vs volume fraction of water ϕ for the system water+(Span 80 +Tween 20)+propanol+oil, benzene (dotted line); toluene (x-x); ethylbenzene (▲); o-xylene (■).

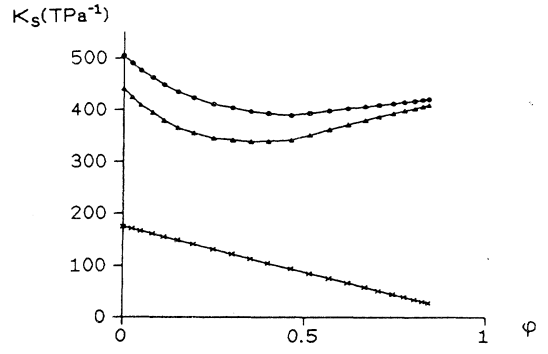

FIG. 7. Variations of K_S (TPa^{-1}) vs volume fraction of water ϕ for the system water+(Span 80+Tween 20)+propanol +benzene, K_S (dotted line) $K_{S,m}$(▲); $K_{S,o}$(x-x).

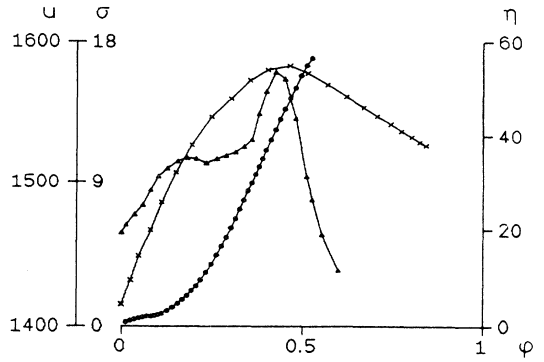

FIG. 8. Variations of conductivity $10^3\sigma$ ($S\,m^{-1}$),. . .; viscosity η (cP), ▲; ultrasonic velocity u(ms^{-1}), x-x; vs volume fraction of water ϕ for the system water+(Span 80+Tween 20)+propanol+benzene.

We can use the ultrasonic velocity u data to characterize the compressional elasticity of the present microemulsions. Ultrasonic velocity can be considered as a thermodynamic zero frequency property related to the density ρ and to the isentropic compressibility K_S of the system by the Laplace relation.

$$K_S = 1/u^2\rho \ . \tag{4}$$

To account for the structural changes, we analyzed the system in terms of the isentropic compressibility K_S (Fig. 7), which is much more sensitive than the velocity to structural changes. Using the same argument as in the case of density, we can compute micellar isentropic compressibility by the equation known as the Wood relation [43–45]

$$K_S = \phi_m K_{S,m} + \phi_o K_{S,o} \ , \tag{5}$$

where $K_{S,o}$ and $K_{S,m}$ are the isentropic compressibility of oil and of micellar phase.

Equation (5) allows us to calculate the $K_{S,m}$ value for each ϕ. As is clear from the table, the compressibility of the micellar phase at $\phi=0$ (anhydrous micelle) is about 441.7 TPa^{-1}. Such a value is much lower than that of the oil ($K_{S,o}=707.7$ TPa^{-1}) but is quite similar to the value of the bulk water ($K_{S,w}=450$ TPa^{-1}).

The comparison of $\rho_m(\phi)$ with $K_{S,m}(\phi)$, reported in Figs. 4 and 7, respectively, reveals surprisingly different trends of the two volumetric properties. Since the $K_{S,m}$ of anhydrous micelles ($\phi=0$) is nearly equal to $K_{S,w}$, it may be inferred that, as ϕ increases and the micelles assume a more waterlike character, $K_{S,m}$ should remain almost constant. On the contrary, the experimental trend of $K_{S,m}(\phi)$ shown in Fig. 7 with a minimum around $\phi=0.45$ ($K_{S,m}=338$ TPa^{-1}) does not conform to such expectation, thus suggesting that the elastic properties of water inside the small droplets are different from those in the bulk water. Such an observation agrees with other reporters [37,46,47] showing modifications in the hydrogen bonded network of water delimited in small constraints. For a high volume fraction of water (ϕ) corresponding to large sizes of droplets $K_{S,m}$ approaches, as expected, towards the compressibility of the bulk water $K_{S,w}$.

IV. CONCLUSION

It may thus be concluded that ρ_m and $K_{S,m}$ results provide some useful information on the structural conditions of the micellar phase in a microemulsion. These exhibit a trend towards an enhanced waterlike character of the dispersed phase. The plot of η, σ, and u in Fig. 8 shows some similarity among the three properties. Below $\phi_c=0.14$, the addition of water results in the creation of a more compact structure with an increasing number of water droplets responsible for the initial increase in ultrasonic velocity and viscosity. It must be emphasized that these conducting droplets, below ϕ_c, do not change much in size (as experimentally demonstrated using neutron scattering by Lagues and Sauterey [20] for a microemulsion system containing sodium dodecyl sulfate as surfactant) and are isolated from each other embedded in a nonconducting continuum oil phase and hence contribute very little to the conductance. At ϕ_c, some of these conducting droplets begin to contact each other and form clusters. The number of such clusters increases very rapidly above the percolation threshold (between $\phi=0.14$–0.45) giving the observed changes in the properties, in particular, the increase in conductivity and ultrasonic velocity. A slight minimum observed in the viscosity behavior may possibly be the result of the rearrangement of rapidly growing droplets forming clusters. At very high $\phi=0.45$ the usual volume expansion property tends to dominate, forming a bicontinuous structure that leads to a decrease in the ultrasonic velocity and viscosity behavior. However, at present, the noncorrelation of the two peaked plots of viscosity with features of other studied physical properties is not clearly understood and thus requires further relevant discussion.

[1] T. P. Hoar and J. H. Schulman, Nature (London) **152**, 102 (1943).
[2] L. M. Prince, *Emulsions and Emulsion Technology,* edited by K. J. Lissant (Marcel Dekker, New York, 1974), Part 1, p. 125.
[3] *Microemulsions Theory and Practice,* edited by L. M. Prince (Academic, New York, 1977).
[4] K. L. Mittal, *Micellization, Solubilization and Microemulsions* (Plenum, New York, 1977).
[5] K. Shinoda and G. Friberg, Adv. Colloid Interface Sci. **4**, 281 (1975).
[6] J. H. Schulman and J. A. Friend, J. Colloid Sci. **4**, 497 (1949).
[7] J. E. Bowcott, J. H. Schulman, Z. Elektrochem. **4**, 283 (1955).
[8] W. Stoeckenius, J. H. Schulman, and L. M. Prince, Kolloid-Z **169**, 170 (1960).
[9] J. Peyrelasse, M. Moho-ouchane, and C. Boned, Phys. Rev. A **38**, 4155 (1988).
[10] Z. Saidi, C. Mathew, J. Peyrelasse, and C. Boned, Phys. Rev. A **42**, 872 (1990).
[11] M. Moho-ouchane, J. Peyrelasse, and C. Boned, Phys. Rev. A **35**, 3027 (1987).
[12] G. S. Grest, I. Webman, S. A. Safran, and A. L. R. Bug, Phys. Rev. A **33**, 2842 (1986).
[13] J. Peyrelasse, C. Boned, and Z. Saidi, Proceedings of the Second European Colloid and Interface Society Conference, Bordeaux, Arcahon, 1988 [Prog. Colloid Polym. Sci. **79**, 263 (1989)].
[14] J. Peyrelasse and C. Boned, Phys. Rev. A **41**, 938 (1990).
[15] N. P. Rao and R. E. Verrall, J. Colloid Interface Sci. **121**, 85 (1988).
[16] S. K. Mehta, R. K. Dewan, and Kiran Bala, Phys. Rev. E **50**, 4759 (1994).
[17] M. Borkovec, H. F. Eicke, H. Hammerich, and B. Das Gupta, J. Phys. Chem. **92**, 206 (1988).
[18] R. L. Read and R. N. Healy, in *Improved Oil Recovery of Surfactant and Polymer Flooding,* edited by D. O. Shah and R. S. Schechter (Academic, New York, 1977), p. 383.
[19] K. E. Bennette, J. C. Hatfield, H. T. Davis, C. W. Macosko, and L. E. Scriven, in *Microemulsion,* edited by I. D. Robb (Plenum, New York, 1982), pp. 65–84.
[20] M. Lagues and C. Sauterey, J. Phys. Chem. **84**, 3503 (1980).
[21] A. M. Cazabat, D. Chatenay, D. Langevin, and J. Meunier, Faraday Discuss. Chem. Soc. **76**, 291 (1982).
[22] D. Chatenay, W. Urbach, A. M. Cazabat, and D. Langevin, Phys. Rev. Lett. **54**, 2253 (1985).
[23] W. Sager, W. Sun, and H.-F. Eicke, Prog. Colloid Polym. Sci. **89**, 284 (1992).
[24] H. F. Eicke, R. Hilfiker, and H. Thomas, Chem. Phys. Lett. **125**, 295 (1986).
[25] S. A. Safran, I. Webman, and G. S. Grest, Phys. Rev. A **32**, 506 (1985); A. L. R. Bug, S. A. Safran, G. S. Grest, and I. Webman, Phys. Rev. Lett. **55**, 1896 (1985).
[26] P. G. de Gennes and C. Taupin, J. Phys. Chem. **86**, 2294 (1982); Y. Talmon and S. Prager, J. Chem. Phys. **69**, 2984 (1978).
[27] S. Bhattacharya, J. P. Stokes, M. W. Kim, and J. S. Huang, Phys. Rev. Lett. **55**, 1884 (1985).
[28] M. A. Van Dijk, Phys. Rev. Lett. **55**, 1003 (1985).
[29] M. Lagues, J. Phys. Lett. **40**, L331 (1979).
[30] M. T. Clarkson, Phys. Rev. A **37**, 2079 (1988).
[31] Y. Song, T. W. Noh, S. I. Lee, and J. R. Gainis, Phys. Rev. B **33**, 904 (1986).
[32] T. J. Coutts, Rev. Thin Solid Films **38**, 313 (1976).
[33] J. P. Straley, Phys. Rev. B **15**, 5733 (1977).
[34] I. Webman, J. Jortner, and M. H. Cohen, Phys. Rev. B **16**, 2593 (1977).
[35] A. L. Efros and B. I. Shklovsku, Phys. Status Solidi **76B**, 475 (1976).
[36] D. M. Grannan, J. C. Gailand, and D. B. Tanner, Phys. Rev. Lett. **46**, 375 (1981).
[37] A. D'Aprano, G. D'Arrigo, A. Paparelli, M. Goffredi, and V. T. Liveri, J. Phys. Chem. **97**, 3614 (1993).
[38] P. D. I. Fletcher, J. Chem. Soc. Faraday Trans. 1 **82**, 2652 (1986).
[39] B. H. Robinson, C. Toprakcioglu, and J. C. Dore, J. Chem. Soc. Faraday Trans. 1 **80**, 13 (1984).
[40] S. H. Chen, T. L. Lin, J. S. Huang, in *Physics of Complex and Supramolecular Liquids,* edited by S. A. Safran and N. A. Clark (Wiley Interscience, New York, 1987).
[41] E. W. Kaler, K. E. Bennette, H. T. Davis, and L. E. Scriven, J. Chem. Phys. **79**, 5673 (1983).
[42] E. W. Kaler, H. T. Davis, and L. E. Scriven, J. Chem. Phys. **79**, 5685 (1983).
[43] L. Ye, D. A. Weitz, P. Sheng, S. Bhattacharya, J. S. Huang, and H. J. Higgins, Phys. Rev. Lett. **63**, 263 (1989).
[44] A. B. Wood, *A Textbook of Sound* (G. Bell, London, 1941).
[45] M. A. Barret-Gultepe, M. E. Gultepe, and E. B. Yeager, J. Phys. Chem. **87**, 1039 (1983).
[46] C. Boned, J. Peyrelasse, and N. Moha-ouchane, J. Phys. Chem. **90**, 634 (1986).
[47] A. Maitra, J. Phys. Chem. **88**, 5122 (1984).